Accepted Manuscript

Reaction Chemistry & Engineering

Linking fundamental chemistry and engineering to create scalable, efficient processes

rsc.li/reaction-engineering

Volume 1
Number 1
1 February 2016
Pages 1-120

PAPER
Timothy Noel et al
A convenient numbering-up strategy for the scale-up of gas-liquid photoredox catalysis in flow

ISSN 2058-9883

ROYAL SOCIETY
OF CHEMISTRY
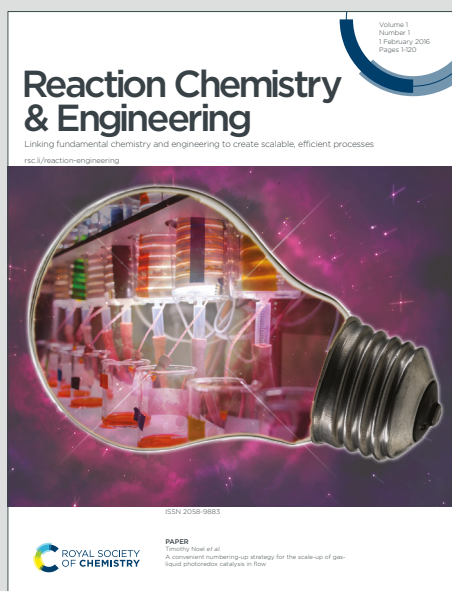
This is an Accepted Manuscript, which has been through the Royal Society of Chemistry peer review process and has been accepted for publication.

Accepted Manuscripts are published online shortly after acceptance, before technical editing, formatting and proof reading. Using this free service, authors can make their results available to the community, in citable form, before we publish the edited article. We will replace this Accepted Manuscript with the edited and formatted Advance Article as soon as it is available.

You can find more information about Accepted Manuscripts in the Information for Authors.

Please note that technical editing may introduce minor changes to the text and/or graphics, which may alter content. The journal's standard Terms & Conditions and the Ethical guidelines still apply. In no event shall the Royal Society of Chemistry be held responsible for any errors or omissions in this Accepted Manuscript or any consequences arising from the use of any information it contains.

ROYAL SOCIETY
OF CHEMISTRY

rsc.li/reaction-engineering

ARTICLE

Kinetic Modelling of Hydrogen Transfer Deoxygenation of a Prototypical Fatty Acid over a Bimetallic Pd$_{60}$Cu$_{40}$ Catalyst: An Investigation of the Surface Reaction Mechanism and Rate Limiting Step

Kin Wai Cheah,[a] Suzana Yusup,[a]* Martin J. Taylor,[b] Bing Shen How,[c] Amin Osatiashtiani,[d] Daniel J. Nowakowski,[d] Anthony V. Bridgwater,[d] Vasiliki Skoulou,[b] Georgios Kyriakou[e] and Yoshitmitsu Uemura[a]

Herein, for the first time, we demonstrate a novel continuous flow process involving the application of tetralin as a hydrogen donor solvent for the catalytic conversion of oleic acid to diesel-like hydrocarbons, using an efficient and stable carbon-supported bimetallic PdCu catalyst. Using Pd$_{60}$Cu$_{40}$/C, where 60:40 is the molar ratio of each metal, at optimum reaction conditions (360 °C and WHSV = 1 h^{-1}), 90.5% oleic acid conversion and 80.5% selectivity to C$_{17}$ and C$_{18}$ paraffinic hydrocarbons were achieved. Furthermore, a comprehensive mechanistic based kinetic modelling - considering power rate law, L-H and E-R models was conducted. Kinetic expressions derived from the three kinetic models were investigated in rate data fitting through nonlinear regression using a Levenberg-Marquardt algorithm. Based on the statistical discrimination criteria, the experimental data of the dehydrogenation reaction of tetralin was best fitted by an L-H rate equation assuming the surface reaction as the rate controlling step. On the contrary, the kinetic data of the oleic acid deoxygenation reaction was well correlated with an L-H rate equation assuming single site adsorption of oleic acid with dissociative H$_2$ adsorption. It was found that the rate limiting step of the overall reaction was the hydrogenation of oleic acid with an activation energy of 75.0 ± 5.1 kJ mol^{-1} whereas the dehydrogenation of tetralin had a lower activation energy of 66.4 ± 2.7 kJ mol^{-1}.

Introduction

Kinetic modelling is a useful tool for chemical process design, optimization and operation of industrial reactors. The knowledge of kinetic parameters not only enables better understanding of the reaction mechanism, but also allows the process to be operated at optimum conditions. Furthermore, catalyst development could benefit from kinetic modelling by studying the overall reaction sequence, rate controlling step and structure-activity relationship, as well as reaction conditions affecting the conversion and product selectivity. Recently, kinetic studies associated to the deoxygenation of fatty acids and triglycerides, currently underutilised compounds found in various waste streams such as cooking residues, waste water effluents and bio-refinery side reactions have received significant attention in the literature.[1, 2] However, as indicated by Boda et al, it is very challenging to obtain conclusive kinetic and mechanistic results from the hydroconversion of plant oils.[3] This is due to heat and mass transfer limitations, which are inevitable in a three-phase reaction of liquid oil and gaseous hydrogen on a solid catalyst. Moreover, plants oils, which are composed of triglycerides and fatty acids with different reactivities, further complicates the kinetic and mechanistic studies. Non-glycerides and fatty acids contaminating components could make the interpretation of the kinetics results dubious as well. Until now, several forms of kinetic models have been proposed to elucidate the reaction mechanism of the catalytic hydrodeoxygenation (HDO) of fatty acids to diesel-like hydrocarbons, a process that we have previously reported using a batch reactor.[4] These models include power-rate law, a Langmuir-Hinshelwood (L-H) model and an Eley-Rideal (E-R) model. Power-rate is the simplest kinetic expression used to fit experimental data without providing any insights into what is occurring on the catalyst surface, while L-H and E-R models are mechanistic-based rate expressions used to investigate the sequential elementary steps in the overall reaction, also to determine the rate-determining step of the reaction.

a. Biomass Processing Laboratory, HICoE – Centre of Biofuel and Biochemical Research, Institute of Self Sustainable Building, Department of Chemical Engineering, Universiti Teknologi PETRONAS, Bandar Seri Iskandar, 32610 Tronoh, Perak, Malaysia. Email: drsuzana_yusuf@utp.edu.my

b. Energy and Environment Institute and Department of Chemical Engineering, University of Hull, Cottingham Road, Hull, HU6 7RX, United Kingdom

c. Chemical Engineering Department, Faculty of Engineering, Computing and Science, Swinburne University of Technology, Jalan Simpang Tiga, 93350 Kuching, Sarawak, Malaysia

d. Energy & Bioproducts Research Institute (EBRI), Aston University, Aston Triangle, Birmingham, B4 7ET, United Kingdom

e. Department of Chemical Engineering, University of Patras, Caratheodory 1, Patras GR 265 04, Greece

Over the past decade, numerous reports have addressed the deoxygenation of fatty acids using model compounds.[5-9] Due to the complexity of mechanistic models, most of the kinetic studies reported in the literature are first order power-rate law. Mechanistic based models like L-H and E-R models are rarely investigated for fatty acid deoxygenation reactions. For instance, Kumar et al. studied the HDO kinetics of stearic acid using n-dodecane as the solvent over $Ni/\gamma-Al_2O_3$.[10] In this work, a comprehensive reaction mechanism was proposed and used to develop a kinetic model based on an empirical first order power law for a HDO reaction. From a non-linear regression algorithm based on Levenberg-Marquardt, the apparent activation energy of stearic acid, as well as C_{15}, C_{16}, C_{17} and C_{18} hydrocarbons were found to be 175.4 kJ mol^{-1}, 387.7 kJ mol^{-1}, 377.2 kJ mol^{-1}, 250.0 kJ mol^{-1} and 190.9 kJ mol^{-1}, respectively. In another power law based kinetic study by Ayodele et al, where a lumped kinetic model based on a simplified reaction mechanism for the HDO of oleic acid was proposed.[11] The authors found that the apparent activation energy was 130.3 kJ mol^{-1}, which is lower than what was found by Kumar et al.[10] In regard to mechanistic based kinetic models, Boda et al investigated the effect of pressure on the HDO of caprylic acid over $NiMo/\gamma-Al_2O_3$ and Pd/C using L-H single site adsorption models.[3] The fatty acid adsorbed on a single active site for the surface reactions while H_2 was found to heterolitically dissociate on a separate site.[3] However, no kinetic parameters were computed for this system. In a recent kinetics study by Zhou & Lawal, the HDO of palmitic acid over 1% $Pt/\gamma-Al_2O_3$ using empirical modelling and mechanistic conjectures including power rate law, L-H and E-R models was carried out.[12] Rate equations derived from power rate law, an L-H mechanism with dual site non-dissociative hydrogen molecules and an E-R model with non-dissociative adsorption of H_2 with non-adsorbed palmitic acid were found to fit the experimental data. The calculated activation energies of power law and E-R were 60.3 kJ mol^{-1}, and the energy observed for the L-H model was found to be 92.9 kJ mol^{-1}.

This study aims to offer an in-depth mechanistic insight into the surface reaction mechanism of the tandem hydrogen transfer-deoxygenation of oleic acid with tetralin as a hydrogen donor source. For the first time, a tandem continuous flow process involving dehydrogenation of tetralin and deoxygenation of oleic acid has been found to be efficiently catalysed over an efficient and stable bimetallic PdCu/C catalyst. By using tetralin as a H donor solvent the necessity to operate high pressure reactors with molecular hydrogen can be negated. Furthermore, carboxylic acids have excellent solubility in tetralin which is used often as a H donor and stabilizing agent in fuel processing.[4] Additionally, Pd-based catalysts are known to be highly effective for the dehydrogenation of tetralin.[4, 13] Unlike previous deoxygenation studies reported in the literature using molecular hydrogen, this kinetic modelling work is a modest attempt to fill the literature gap, where no recent efforts have been attempted in elucidating the surface reaction mechanism of the hydrogen transfer-deoxygenation of oleic acid using an in-situ produced hydrogen source. The kinetic modelling study builds on our previous work in which we

screened a series of $Pd_xCu_{(1-x)}$ bimetallic catalysts supported on activated carbon and assessed the effect of Pd dilution and PdCu synergetic behaviour in a batch reactor.[4] It was demonstrated that the $Pd_{60}Cu_{40}/C$ catalyst exhibited excellent catalytic performance in converting oleic acid into diesel paraffinic hydrocarbons. The bimetallic material proved to be superior to monometallic Pd/C. However, the surface reaction mechanism and individual role of the active site (Pd & Cu) in the catalytic deoxygenation of oleic acid were yet to be clarified. In this work we focus on (i) studying the effect of reaction temperatures and weight hourly space velocity (WHSV) on the reactants conversion and diesel hydrocarbon selectivity, (ii) developing a mechanistic insight into the surface reactions and (iii) determining the rate-limiting step of the overall reaction.

Material and Methods

All the protocols related to the synthesis and characterisation of the $Pd_{60}Cu_{40}/C$ catalyst, created in the absence of capping agents e.g. PPh$_3$, PVP or PVA to negate residual catalyst surface decoration.[14, 15] A summary of physicochemical properties of this catalyst can be found in our previous work and **Table S1**.[4] Methods for development and fitting of the mathematical kinetic equations are also presented in the supporting Information.

Experimental setup

In this work, the catalytic hydrogen transfer deoxygenation of oleic acid ($C_{18}H_{34}O_2$, Technical grade 90%, Sigma-Aldrich) with tetralin ($C_{10}H_{12}$, anhydrous 99%, Sigma-Aldrich) was performed in a custom-made stainless steel 316 unit continuous tubular fixed-bed reactor, (Amar Equipments Pvt Ltd, Mumbai, India) with an internal diameter of 35 mm and length of 500 mm. **Figure 1** shows the schematic flow diagram of the continuous tubular fixed-bed reactor system, which consists of a feed unit, a pre-heating unit, a reactor unit and a product separation unit. The gas feed assembly has two gas inlets for H_2 and N_2, where the flow rate of both gases were controlled via mass-flow controllers (Brooks, 5850E). For the liquid feed assembly, a stainless steel feed vessel with a 1 L capacity was connected to a HPLP pump (Lab Alliance series SSI) via a ½ inch stainless steel tube equipped with a 10-inline 60 µm filter. The liquid was fed by the piston-bearing pump through the pre-heater unit. The homogeneous gas mixture was then flowed co-currently downward into the reactor unit. The tubular reactor was heated electrically with a split tube two zone furnace. It was also equipped with a K-type thermocouple placed inside a thermowell used to monitor the temperature profile of the reactor. The temperature was controlled by two controllers situated at the top and bottom of the reactor. The catalyst sample was positioned in the middle of the reactor to keep it within the optimal heating zone. The pressure inside the reactor was regulated by using a manual back pressure regulator (TESCOM Control Pressure Regulator, 26-1700 Series) located downstream from the condenser. The outlet stream of the reactor was directed to a shell and tube condenser, in which the products were cooled by circulating water. The gas and liquid

mixture were then separated in a double jacket water cooled separator.
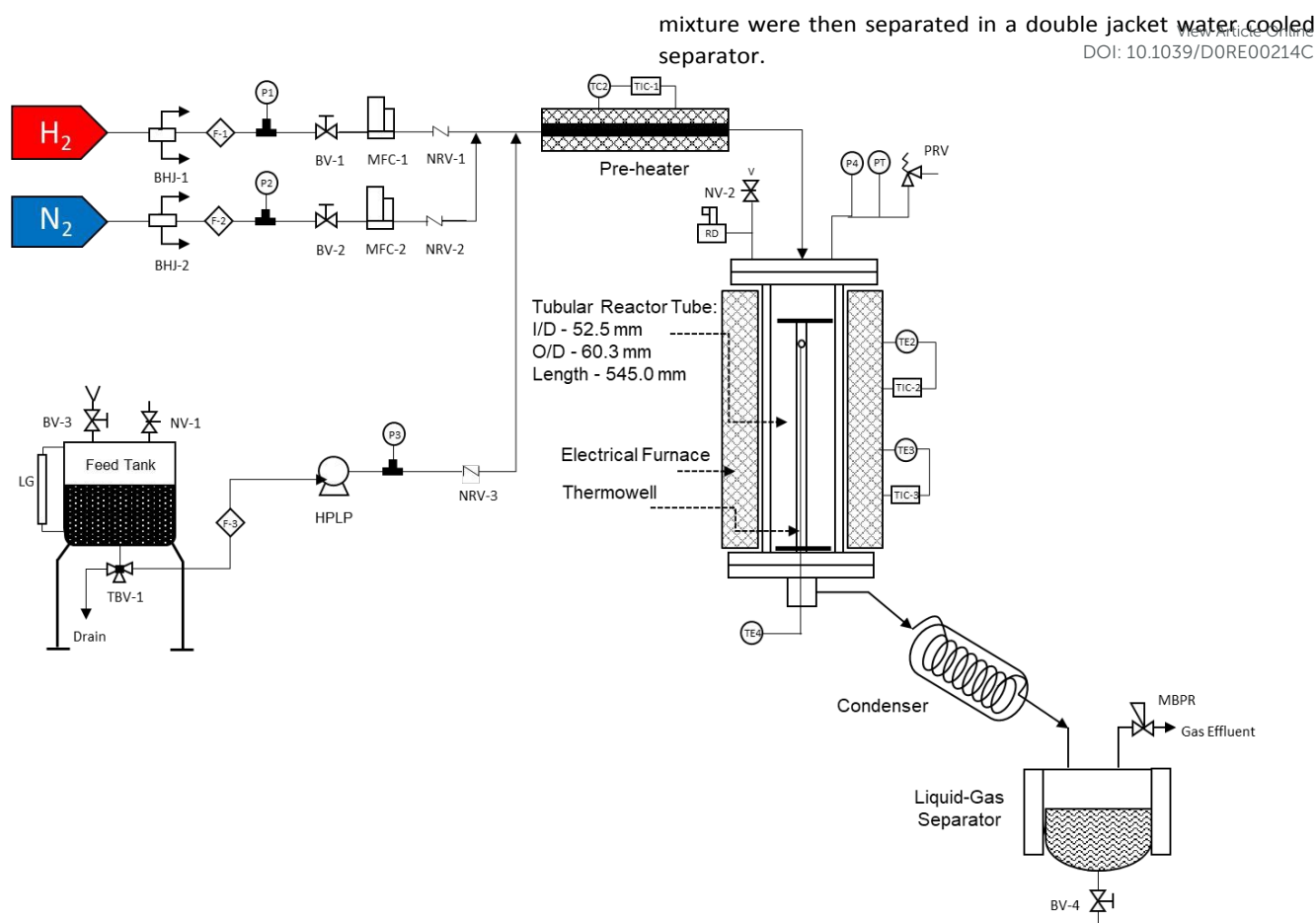
Figure 1: Schematic diagram of the continuous tubular fixed-bed reactor system. LG: Level Gauge, TE: Temperature Element (TE1-TE4), TIC: Temperature Indicator/Controller (TIC-1 to TIC-3), P: Pressure Gauge, F: Filter (F-1 to F-3), BV: Ball Valves (BV-1 to BV-3), PRV: Pressure Safety Valve; MBPR: Manual Back Pressure Regulator, NV: Needle Valve (NV-1 to NV-2), NRV: Non Return Valve (NRV-1 to NRV-3), RD: Rupture Disc, MFC: Mass Flow Controller (MFC-1 to MFC-2), BHU: Bulk Head Union (BHU-1 and BHU-2).

Catalytic testing

Prior to any experiment the reactor and gas-liquid separator were washed thoroughly with n-hexane to remove any contaminants and residues, this was followed by purging with flowing N_2 at 100 mL min^{-1} for 0.5 h. Catalyst samples were dried overnight at 105 °C to remove any trapped moisture. The dried catalyst (0.5–3.5 g) was positioned between two layers of quartz wool which acted as a phase distributor over the reactor cross-section, also to keep the catalyst in position during the reaction. Next, the catalyst was reduced in-situ at 450 °C for 3 h with 50 mL min^{-1} of flowing H_2 gas. Subsequently, the excess H_2 was removed by a N_2 purge at 100 mL min^{-1} for 1 h. The reactor was then pressurized with N_2 gas up to 1 MPa and heated to the desired reaction temperature. While the reactor was heating, the outlet valve of the gas-liquid separator was opened several times to remove any residual hexane from the system, avoiding product contamination. Once the reaction temperature and pressure were equilibrated, the oleic acid and tetralin feed mixture (mass ratio of 1:1) was introduced continuously into the reactor through the catalyst bed and the volumetric flow rate of the gas was regulated by a mass flow controller. A set of experiments were conducted under different operating conditions to determine the kinetic rate expression of deoxygenation of oleic acid with tetralin. Reaction temperature and WHSV were varied in the range of 300–390 °C and 1–10 h^{-1}, respectively. WHSV is defined as the weight of the liquid feed flowing per unit of the catalyst per hour. Liquid samples were withdrawn from the bottom of gas-liquid separator hourly with a total of 7 h per run.

Product analysis

The liquid products were analysed using an Agilent 7820A Gas Chromatograph with a Flame Ionization Detector (FID) fitted with a HP-5 (5%-phenyl-95%-dimethylpolysiloxane) capillary column (length, 30 m; internal diameter, 0.32 mm; film thickness, 0.25 μm) and an 8400 auto-sampler. The initial temperature of the column was set at 60 °C. The oven temperature was then ramped up at a rate of 20 °C min^{-1} to 300 °C for 2 min. The liquid product sample (100 μL) was diluted in 900 μL of toluene. Quantitative calculations were carried out by using mesitylene as an external standard. The liquid products were further validated using an Agilent 7890A Gas Chromatograph equipped with a Quadrupolar Mass Spectrometer (QMS). Acquired mass spectra were compared with the National Institute of Standards and Technology (NIST)

ARTICLE

mass spectral library. The product gas was collected in a sealed gas bag and analysed using an Agilent 7820 GC with a Thermal Conductivity Detector (TCD) and a 10' (3 m) column containing 100/120 mesh Carbonsieve S-11 spherical carbon packing. In this work, oleic acid and tetralin conversion, as well as diesel hydrocarbon selectivity were defined as follows:

$$X_{TET}\ (\%) = \left(\frac{TET_{in} - TET_{out}}{TET_{in}}\right) \times 100$$

$$X_{OA}\ (\%) = \left(\frac{OA_{in} - OA_{out}}{OA_{in}}\right) \times 100$$

$$C_{17-18}\ selectivity\ (\%) = \frac{C_{17-18}}{OA_{in} - OA_{out}} \times 100$$

Where TET_{in} is the molar concentration of tetralin entering the reactor, TET_{out} is the molar concentration of tetralin exiting the reactor, OA_{in} is the molar concentration of oleic acid entering the reactor, OA_{out} is the molar concentration of oleic acid exiting the reactor, C_{17-18} is the molar concentration of C_{17}-C_{18} hydrocarbons formed during the reaction.

Results & Discussion

External/Internal mass transfer limitation

The heterogeneous hydrogen transfer deoxygenation of oleic acid over a bimetallic $Pd_{60}Cu_{40}$/C catalyst involved the liberation and adsorption of hydrogen atoms from a donor solvent, some of which recombine producing molecular hydrogen which transitions through a liquid-gas phase boundary layer surrounding the external catalyst surface. As the mass transfer rate is usually affected by flow velocity, the impact of overall external mass transfer were evaluated experimentally by studying the change of Space-Time-Consumption (STC) of oleic acid and tetralin at different N_2 gas flow rates (50-200 mL min⁻¹) and liquid flow rates (0.1– 0.2 mL min⁻¹) under similar experimental conditions, by keeping the solvent to fatty acid mass ratio, reaction temperature, WHSV and reaction pressure constant at 1, 300 °C, 10 h⁻¹ and 1 MPa, respectively. In this work, superficial flow velocity is expressed as follow:

$$V_f = \frac{Q_{Total}}{A}$$

Where V_f is the superficial flow velocity, Q_{Total} is the total volumetric flow rate and A is the cross sectional area of reactor.

Figure S1 shows the effect of superficial flow velocity on STC of oleic acid and tetralin. The results indicated that the STC of oleic acid and tetralin were independent of superficial flow velocity in the studied range of 1.0×10^{-3} ms⁻¹ to 3.5×10^{-3} ms⁻¹. In other words, both reactions do not appear to be limited by external mass transfer, even at the lowest superficial flow velocity of 1.0×10^{-3} ms⁻¹. This indicates that, at the lowest velocity

selected in this study, the liquid-gas phase boundary layer was so thin that it no longer exhibited resistance to external diffusion, hence reactions under these conditions were not limited by the external mass transfer. As a result, the lowest flow velocity of 1.0×10^{-3} ms⁻¹ was chosen as the baseline velocity for the kinetic studies.

Even though the heterogeneous deoxygenation reaction is free from external mass transfer limitations, it is still possible that the reaction is controlled by internal mass transfer. Internal mass transfer limitation occurs when the reactants exhibit slow diffusion rate from the pore entrance to the internal porous network of the catalyst. This is due to the existence of a significant concentration gradient between the porous apertures to the internal areas. Internal mass transfer effects were evaluated by calculating the Wiesz-Prater parameter and can be neglected when the following relationship holds.

$$C_{wp} = \frac{-r'_{OA\ (obs)}\rho_p R^2}{D_e C_{As}} < 1$$

$$D_e = \frac{D_{AB}\varphi_p\sigma_c}{\tau}$$

Where C_{wp} is the Weisz-Prater parameter, $-r'_{OA\ (obs)}$ is the observed reaction rate, ρ_p is the density of the catalyst, R is the characteristic diameter of the catalyst, C_{As} is the hydrogen concentration at the external surface of catalyst, D_e is the effective diffusivity of hydrogen into the catalyst, D_{AB} is the binary diffusivity of hydrogen in oleic acid, ϕ_P is the catalyst porosity, σ_C is the catalyst constriction factor and τ is catalyst tortuosity.

The binary diffusivity of molecular hydrogen in oleic acid can be calculated by using the Wilke-Chang correlation equation, as shown below:[16]

$$D_{AB} = \frac{7.4 \times 10^{-8} \times (\phi\ M_B)^{0.5} \times T}{\eta_B \times V_A^{0.6}}$$

Where A and B refer to the concentration of molecular hydrogen and oleic acid, D_{AB} is the binary diffusivity of molecular hydrogen in oleic acid, M_B is the molecular weight of oleic acid, T is reaction temperature, η_B is the viscosity of oleic acid, V_A is the molar volume of hydrogen at its normal boiling point and ϕ is the association factor of oleic acid.

The molar volume of oleic acid can be estimated by using the equation below, where V_c is the critical volume of oleic acid, 1152 cm³ mol⁻¹.[17]

$$V_A = 0.285 \times V_C^{1.048}$$

The average catalyst grain radius was 5 μm after grinding. The bulk density of the $Pd_{60}Cu_{40}$/C catalyst was calculated experimentally and found to be 0.45 g mL⁻¹. The observed rate of reaction at 300 °C was 1.31×10^{-6} mol s⁻¹ g⁻¹$_{cat}$. Using the Wilke-Change correlation, the effective binary diffusivity of

molecular hydrogen in oleic acid was estimated to be 6.2 x 10^{-5} mol m^{-3}. Using the typical reported values for porosity, constriction factor and tortuosity of 0.5, 0.8 and 3, respectively. The Weisz-Prater parameter (C_{wp}) at the lowest temperature (300 °C) was found to be 0.437, which corresponds to an internal effectiveness factor of unity.[12, 18] This indicates that the actual overall rate of reaction is less than the diffusion rate, and thus it can be concluded that the rate of reaction was not kinetically controlled by internal mass transfer. This is due to the low porosity of the catalyst, as shown in in our previous work and in **Table S1**.[4]

Heat transfer limitation

Apart from mass transfer limitations, many previous publications reported that poor heat transfer characteristics resulted in significant temperature variation in the reactor, this causes the reaction to occur at different rates and mask the true kinetics of the reaction. To determine whether there are any heat transfer limitations in any domains, Biot number (Bi), defined as the ratio of thermal resistance of the particle to that of the film around the particle, was calculated.

$$Bi = \frac{hd_p}{\lambda}$$

Where h is the heat transfer coefficient, d_p is the diameter of the catalyst grain and λ is the effective thermal conductivity of a porous catalyst. The Biot number was found to be 0.001, which implies that the effect of interparticle heat transfer resistance is predominant over the interphase or intraparticle heat transport resistance. Interparticle heat transport can occur radially and axially within the reactor.

The radial heat transfer effects were evaluated by the following Damkohler number (D_a), equation:

$$D_a = \left| \frac{-\Delta H\,(-R_{obs})(1-\varepsilon)R_0^2}{\lambda T_w(1+b)} \right| < 0.4 \frac{RT_w}{E_a}$$

Where ΔH is the heat of reaction in J mol-1, Robs is the observed rate of reaction, ε is the bed porosity, Ro is the internal radius of the reactor, b is the ratio of diluent to catalyst volume, E_a is the activation energy in J mol^{-1}.

In this work, the axial heat transport limitation effect can be considered to be negligible due to the fact that the ratio of axial length of the reactor (0.5 m) to the catalyst grain size (10 μm) was much greater than 20. Axial heat transfer effect can be considered insignificant if the ratio of axial length of the reactor to the catalyst grain size is greater than 20. The radial heat transport effect was evaluated by calculating the Damkohler number (D_a) and comparing it to the value of 0.4(RT$_w$/E$_a$). The heat of reaction was calculated to be 35.3 x 10^3 J mol^{-1} and the observed reaction rate at 300 °C was 0.586 mol m^{-3} g^{-1}cat. The internal radius of the flow reactor was 0.018 m and the activation energy obtained was 75.0 x 10^3 J mol^{-1}. In this work, the calculation showed that the left side of the equation

(0.0077) was an order of magnitude smaller than the right side of the equation (0.024), indicating that the radial temperature difference in the reactor was less than 5 % of the average cross sectional temperature.[12, 18] Thus, it can be concluded that radial heat transfer effect was not a limiting factor in the reactor. In summary, based on the mass and heat transfer analysis, the kinetic study experiments were not conducted in the heat and mass transfer controlling regime.

Reaction equilibrium

Figure S2 and **Figure S3** show the catalytic stability of Pd$_{60}$Cu$_{40}$/C catalyst in the deoxygenation of oleic acid with tetralin in a continuous fixed bed reactor over 7 h. As shown in **Figure S3**, the conversion of oleic acid dropped rapidly during the first 2 h of the reaction and then reached a plateau, whereas tetralin conversion (**Figure S2**) reached steady-state conversion within 1 h. The initial upsurge in the catalytic activity at the first hour followed by a steady state is in agreement to the reaction profile observed by Zhou & Lawal using a Pt/C catalyst.[12] It was reported that the fresh Pt based catalyst was initially highly active for the first hour, before declining and maintaining a stable catalytic performance after 4-5 h time-on-stream The Pd$_{60}$Cu$_{40}$/C catalyst retained its activity, even after 7 h of reaction, suggesting there is no catalyst deactivation under the conditions used in this study. This could be explained by the presence of excess molecular hydrogen liberated from tetralin, preventing surface oxidation of the Pd and Cu sites.[17] With the sustained activity while on stream, it can be concluded that the reaction system achieved equilibrium conditions with not more than 10% deviation from the average conversion performance.

Catalyst Reactivity

The effect of reaction temperature and WHSV on oleic acid and tetralin conversion as well as product selectivity over the Pd$_{60}$Cu$_{40}$/C catalyst was investigated at different temperatures in the range of 300-390 °C and WHSVs between 1 and 10 h^{-1}. **Table 1** summarizes the catalytic activity of Pd$_{60}$Cu$_{40}$/C in a fixed-bed continuous flow reactor over 7 h. From **Table 1**, it can be clearly observed that increasing the reaction temperature leads to an increase in the conversion of oleic acid and tetralin. The conversion of tetralin and oleic acid were found to be ~64% at 300 °C and WHSV = 1 h^{-1}. With increasing reaction temperature, the conversion of both reactants was nearly completed (X_{OA} = 91.4% and X_{TET} = 95.3%, respectively) at 390 °C and 1 h^{-1}. It is worth noting that the viscosity of oleic acid reduces with an increase in reaction temperature.[11, 19] This enhances the solubility of H_2 molecules into the liquid phase and its propensity into the reaction mixture, hence improving the diffusional mass transfer of H_2 in the reaction mixture. The increasing trend of both reactant conversions also indicates that both deoxygenation of oleic acid and dehydrogenation of tetralin reactions are in accordance with the well-established Arrhenius theory of temperature dependence of reaction rates. Moreover, the impact of WHSV on the catalytic reactivity was investigated by varying the catalyst charge (0.5–3.5 g) and keeping the feed rate constant. From **Figure 2(a)** and **Figure 2(b)**, it was found that the conversion of both reactants

ARTICLE

Journal Name

decreased linearly with an increasing WHSV. This can be explained in terms of shorter contact time between the reactant molecules and the catalyst surface.

Furthermore, the reaction mixture analysis revealed that stearic acid, n-heptadecane (C_{17}) and n-octadecane (C_{18}) were the main products of the reaction. No heptadecene was detected in the liquid products, this suggests that either the C_{17} alkene is spontaneously hydrogenated as it is formed, or the decarbonylation pathway is less favourable.[4] **Figure 2(c)** demonstrates the dependency of saturated C_{17} and C_{18} hydrocarbon selectivity on the reaction temperature and WHSV. Across all the WHSVs, the selectivity towards saturated hydrocarbons reached a maximum at 360 °C where C_{17} was the major product, indicating that both decarboxylation and hydrodeoxygenation reaction pathways are favoured at this temperature.[9, 20] Further increasing the reaction temperature to 390 °C resulted in enhanced stearic acid selectivity, a switch from C_{17}-C_{18} alkanes, suggesting that the hydrogenation of oleic acid to stearic acid is the dominant reaction pathway compared to the HDO of stearic acid. This could be explained by the exothermic nature of the decarboxylation reaction, previously shown to have a ΔH value of -23.5 kJ mol^{-1}.[21] As the reactor temperature was increased to 390 °C, the prevailing reaction equilibrium was upset due to the external thermal stress

applied on the system. With the additional thermal stress present within the reaction system, a new dynamic reaction equilibrium was formed. The equilibrium shifted to the reverse endothermic direction to partially offset the effect of thermal stress applied, producing more steric acid. Further elevation in reaction temperature will remarkably inhibit the deoxygenation reaction and reduce the diesel hydrocarbon selectivity. Such phenomena are in good agreement with the fundamental Le-Chatelier's principle, where an increase in the reaction temperature of an exothermic reaction will shift the equilibrium to the reverse direction. On the other hand, in the reaction temperature range investigated in this work, the selectivity of n-octadecane was observed to be improved monotonically, as shown in **Figure 2(c)**. Such small increments in n-octadecane's selectivity could be attributed to the excess H present on the catalyst surface after the dehydrogenation of tetralin. The hydrogen-rich environment promoted the conversion of stearic acid into n-octadecane, rather than the decarboxylation reaction. Previous studies have reported that a high hydrogen partial pressure favours the production of n-octadecane via a HDO reaction opposed to the decarboxylation reaction pathway.[22]

Table 1: Reactant conversions and products selectivity for the hydrogen transfer deoxygenation of oleic acid using tetralin as an in-situ H donor at various reaction temperatures and WHSVs. (Reaction conditions: oleic acid concentration = 3.6 mol L^{-1}, oleic acid:tetralin mass ratio = 1 , catalyst mass = 0.5 g–3.6 g , TET = Tetralin, OA = Oleic acid, SA = Stearic acid, C_{17} = Heptadecane, C_{18} = Octadecane

	300 °C					330 °C				
WHSV	**X %**		**Selectivity %**			**X %**		**Selectivity %**		
h[-1]	**TET**	**OA**	**SA**	**C_{17}**	**C_{18}**	**TET**	**OA**	**SA**	**C_{17}**	**C_{18}**
1	64	63	45	51	4	74	81	26	70	4
2.5	50	49	60	38	2	58	59	39	58	3
5	26	26	78	21	1	43	46	61	37	2
10	11	12	87	14	0	25	23	80	20	0
	360 °C					**390 °C**				
WHSV	**X %**		**Selectivity %**			**X %**		**Selectivity %**		
h[-1]	**TET**	**OA**	**SA**	**C_{17}**	**C_{18}**	**TET**	**OA**	**SA**	**C_{17}**	**C_{18}**
1	86	91	20	75	6	91	95	50	40	10
2.5	72	77	29	66	5	87	82	56	37	7
5	49	50	47	50	3	64	59	60	35	5
10	31	33	68	33	0	41	41	74	25	1

(a) **(b)** **(c)**
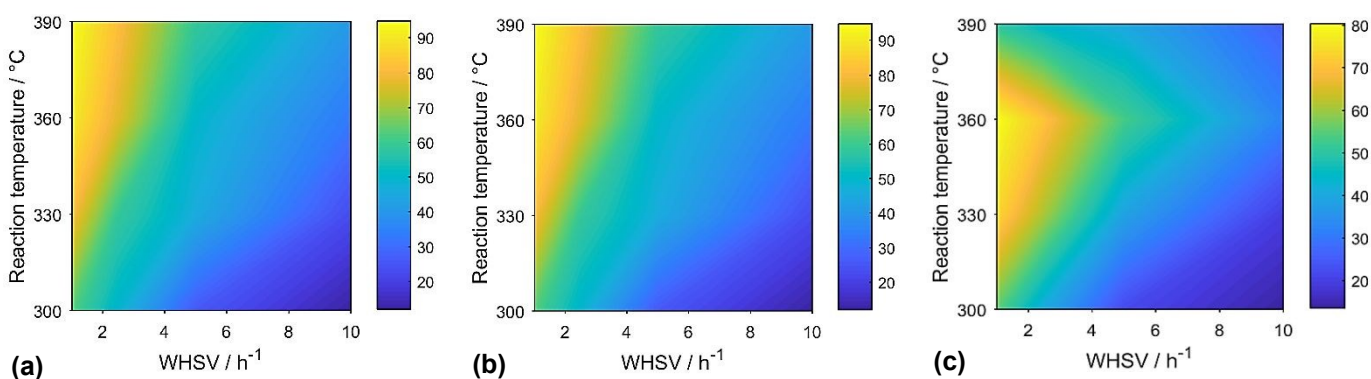
Figure 2: **(a)** Tetralin conversion, X_{TET}, **(b)** Oleic acid conversion, X_{OA} and **(c)** Selectivity of C_{17} and C_{18} saturated hydrocarbons, C_{17}+C_{18} in hydrogen transfer deoxygenation of oleic acid using tetralin as hydrogen source (Reaction conditions: oleic acid concentration = 3.6 mol L^{-1}, oleic acid:tetralin mass ratio = 1, catalyst mass = 0.5-3.6g)

ARTICLE

Power law, L-H and E-R models

Based on our earlier work,[4] tetralin dehydrogenation (**Reaction 1**) and oleic acid deoxygenation (**Reaction 2**) occur sequentially over the bimetallic $Pd_{60}Cu_{40}/C$ catalyst. The tandem hydrogen transfer dehydrogenation reaction consists of three consecutive surface reactions: **(i)** hydrogen atom production from the dehydrogenation of tetralin, **(ii)** hydrogenation of oleic acid (OA) to stearic acid (SA) using the in-situ produced hydrogen and **(iii)** decarboxylation of stearic acid to heptadecane (C_{17}).

In order to determine the rate limiting step of the tandem reaction system, three type of rate equations including power rate law kinetics, L–H and E–R mechanistic conjuncture models were developed and derived as presented in **Table 2**. Where, r_1 and r_2 are the rate of **Reaction 1** and **2**, respectively and $k_{rxn,1}$ and $k_{rxn,2}$ specify the rate constants of **Reaction 1** and **Reaction 2**, respectively. k_x is the adsorption equilibrium constant of chemical species X and [X] is the outlet molar concentration of chemical species X. The detailed derivation steps for the kinetic models can found in the supplementary information.

A simple power rate law kinetic model is used as the elementary reaction model to describe the dependence of reaction rate on temperature and reactant concentration. In this work, the rate of reaction was expressed in terms of the concentration of oleic acid, tetralin and produced hydrogen atoms raised to the experimentally determined exponents (α and β), respectively (R1-(A) and R2-(A)). However, this quick approach does not provide any insight into what is occurring on the catalyst surface.

Other than the power rate law model, a more detailed mechanistic conjuncture model, Langmuir Hinshelwood (L-H) was used to describe a bimolecular surface reaction between two adsorbed reactant species on the catalytic active site, S. In L-H models, two reactant species of interest (oleic acid and reactive hydrogen atoms) are assumed to be firstly adsorbed on the active site at the surface of the catalysts, followed by an irreversible, rate determining surface reaction to form products. The L-H surface reaction mechanism can be categorized into two types: (i) single site adsorption and dual site adsorption. In the single site adsorption model, both reactant species assume to be adsorbed competitively on the same active site (S) before reaction. While for the (ii) dual adsorption model, the reactant species will adsorb non-competitively and independently on two different active sites (S_1 and S_2).

It is worthwhile to note that the hydrogen atoms liberated from tetralin in a single step could be adsorbed on the active sites in the form of a dissociative hydrogen atom (H) or recombine generating non-dissociative molecular hydrogen (H_2) which can desorb to the gas phase, followed by potential readsorption. As a result, a total combination of 8 L-H based surface reaction models (R2-B to R2-I) were developed and derived for **Reaction 2** as listed in **Table 2**.

Another mechanistic conjuncture model, E-R, was also taken into account by only assuming a single reactant species adsorbed onto the catalyst surface with another reactant species in the gas phase. For the E-R kinetic models, we assumed the adsorption of oleic acid with non-adsorbed hydrogen molecules from the liquid phase (R2-J) and non-adsorption of oleic acid with dissociative adsorption of hydrogen atoms, H_{ads} (R2-K).

Table 2: Rate equations derived for Power Law, L-H and E-R surface reaction models.

Reaction	No.	Type of surface reaction model	Rate equation
Reaction 1	R1(A)	Power Law model with tetralin dehydrogenation	$r_1 = k_{rxn,1}[TET]^\alpha$
	R1(B)	L-H model with single site adsorption of tetralin $TET*S \rightarrow Nap*S + 4H$	$r_1 = \dfrac{k_{rxn,1}k_{TET}[TET]}{(1 + k_{TET}[TET])}$
Reaction 2	R2(A)	Power Law model with oleic acid deoxygenation	$r_2 = k_{rxn,2}[OA]^\alpha[H_2]^\beta$
	R2(B)	L-H model with single site adsorption of oleic acid with H_2 $OA*S + H_2*S \rightarrow SA*S + S$	$r_2 = \dfrac{k_{rxn,2}\,k_{OA}[OA]\,k_{H_2}[H_2]}{(1 + k_{OA}[OA] + k_{H_2}[H_2])^2}$
	R2(C)	L-H model with single site adsorption of stearic acid with H_2 $SA*S \rightarrow C17*S + CO_2$	$r_2 = \dfrac{k_{rxn,2}\,k_{SA}k_{OA}[OA]k_{H_2}[H_2]}{(1 + k_{OA}[OA] + k_{H_2}[H_2] + k_{SA}k_{OA}[OA]k_{H_2}[H_2])}$
	R2(D)	L-H model with single site adsorption of oleic acid with H atoms $OA*S + 2H*S \rightarrow SA*S + 2S$	$r_2 = \dfrac{k_{rxn,2}\,k_{OA}[OA]\,k_{H_2}[H_2]}{\left(1 + k_{OA}[OA] + \sqrt{k_{H_2}[H_2]}\right)^3}$
	R2(E)	L-H model with single site adsorption of stearic acid with H atoms $SA*S \rightarrow C_{17}*S + CO_2$	$r_2 = \dfrac{k_{rxn,2}\,k_{SA}k_{OA}[OA]k_{H_2}[H_2]}{\left(1 + k_{OA}[OA] + \sqrt{k_{H_2}[H_2]} + k_{SA}k_{OA}[OA]k_{H_2}[H_2]\right)}$
	R2(F)	L-H model with dual site adsorption of oleic acid with H_2 $OA*S_1 + H_2*S_2 \rightarrow SA*S_1 + S_2$	$r_2 = \dfrac{k_{rxn,2}\,k_{OA}[OA]\,k_{H_2}[H_2]}{(1 + k_{OA}[OA])(1 + k_{H_2}[H_2])}$

R2(G)	L-H model with dual site adsorption of stearic acid with H_2 $SA * S_1 \rightarrow C_{17} * S_1 + CO_2$	$r_2 = \dfrac{k_{rxn,2}\, k_{SA}k_{OA}[OA]k_{H_2}[H_2]}{(1 + k_{OA}[OA] + k_{SA}k_{OA}[OA]k_{H_2}[H_2])}$
R2(H)	L-H model with dual site adsorption of oleic acid with H atoms $OA * S_1 + 2H * S_2 \rightarrow SA * S_1 + 2S_2$	$r_2 = \dfrac{k_{rxn,2}\, k_{OA}[OA]\, k_{H_2}[H_2]}{(1 + k_{OA}[OA])\left(1 + \sqrt{k_{H_2}[H_2]}\,\right)^2}$
R2(I)	L-H model with dual site adsorption of stearic acid with H atoms $SA * S_1 \rightarrow C_{17} * S_1 + CO_2$	$r_2 = \dfrac{k_{rxn,2}\, k_{SA}k_{OA}[OA]k_{H_2}[H_2]}{(1 + k_{OA}[OA] + k_{SA}k_{OA}[OA]k_{H_2}[H_2])}$
R2(J)	E-R model with adsorbed oleic acid and non-adsorbed H_2 $OA * S + H_2 \rightarrow OA * S$	$r_2 = \dfrac{k_{rxn,2}k_{OA}[OA][H_2]}{(1 + k_{OA}[OA])}$
R2(K)	E-R model with non-adsorbed oleic acid and adsorbed H atoms $2H * S + OA \rightarrow SA * 2S$	$r_2 = \dfrac{k_{rxn,2}\, k_{H_2}[OA]\,[H_2]}{\left(1 + \sqrt{k_{H_2}[H_2]}\,\right)^2}$

Evaluation of model discrimination

As the catalytic reaction was performed over a continuous tubular packed bed reactor, the reaction rates of **Reaction 1** and **Reaction 2** are determined using the outlet molar flow rate of unreacted oleic acid and tetralin species per unit mass of $Pd_{60}Cu_{40}/C$ used. In this work, the outlet molar flow rate of oleic acid and tetralin at exit are defined as below:

$$F_{TET,out} = TET_{out} \times F_{in}$$

$$F_{OA,out} = OA_{out} \times F_{in}$$

Where $F_{TET,out}$ is the outlet molar flow rate of tetralin, $F_{OA,out}$ is the outlet molar flow rate of oleic acid, TET_{out} is the molar concentration of tetralin exiting the reactor, OA_{out} is the molar concentration of oleic acid exiting the reactor and F_{In} is the liquid flow rate entering the reactor.

By plotting $F_{OA,out}$ and $F_{TET,out}$ against w, the reaction rates were found to follow an exponential manner with R_2 close to unity as shown in **Figure 3** and **Figure 4**, respectively. This indicates that the regression predictions fit the experimental data closely. The reaction rate of each temperature can be calculated by numerically differentiating the corresponding exponential functions obtained. The consumption rate of oleic acid and tetralin were then substituted into the rate equations derived from the proposed reaction kinetics models. From each kinetic model, the individual rate equation was subjected to a non-linear regression analysis paired with the Levenberg-Marquardt algorithm in the
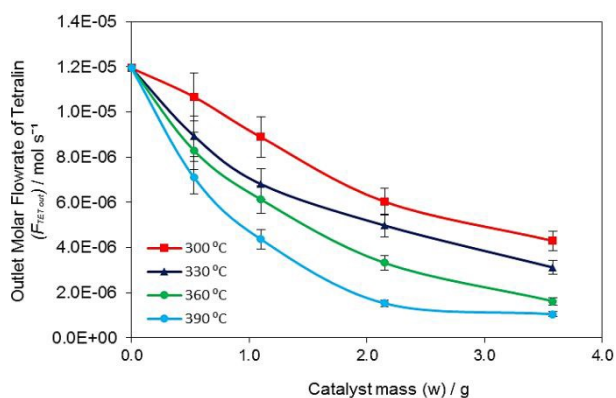
MATLAB software. In order to determine the kinetic constants, the rate data was fitted and solved by system optimization in a way that the error difference between the experimental and predicted value is minimized. The discrimination among the rival models with a surface reaction as rate limiting steps were based on the criteria that all the kinetic constants must be positive, R^2 must be greater than 0.95 and the RMSE value should be minimal.

For the dehydrogenation of tetralin (**Reaction 1**), it was found that the kinetic data was best fitted by the L–H rate equation derived for the surface reaction as the rate controlling step, evident from its high degree of accuracy represented by its R^2 value and low RMSE value as shown in **Table S2**. In contrast, power-law model was also found to be a poor fit with R^2 values <0.95. The pseudo-first order model also possesses fairly large RMSE values, as compared to the L–H model. Therefore, due to its low accuracy, it was not considered. Regarding the deoxygenation of oleic acid (**Reaction 2**), four rate equations derived from the L–H mechanistic model with the assumption of (i) single site adsorption of stearic acid with (ii) single site adsorption of oleic acid and liberated H atoms from **Reaction 1**, (iii) dual site adsorption of oleic acid and non-dissociative H_2 and (iv) dual site adsorption of oleic acid and dissociative H atoms were found to fit the experimental rate data well with an R^2 > 0.95. Among the four L-H mechanistic models, the RMSE values of single site adsorption model of oleic acid with dissociative hydrogen atoms was found to be the smallest compared to the others three L-H mechanistic models. Therefore, both dual site L-H mechanistic models and the

Figure 3: Outlet molar flow rate of tetralin as a function of catalyst mass at different reaction temperatures. (Reaction conditions: oleic acid concentration 3.6 mol L⁻¹, oleic acid:tetralin mass ratio = 1, catalyst mass = 0.5 - 3.6 g , N_2 pressure = 1 MPa).
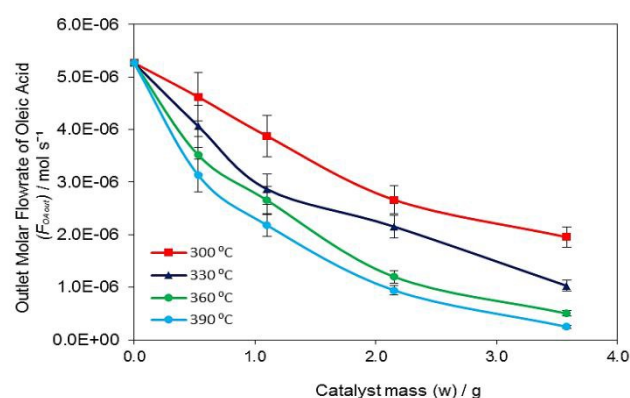
Figure 4: Outlet molar flow rate of oleic acid as a function of catalyst mass at different reaction temperatures. (Reaction conditions: oleic acid concentration = 3.6 mol L⁻¹, oleic acid:tetralin mass ratio = 1, catalyst mass =0.5 - 3.6 g , N_2 pressure = 1 MPa)

Journal Name

ARTICLE

single site adsorption model of stearic acid were not considered for further data processing. Based on the discrimination constraints, the kinetic data of **Reaction 2** was best fitted by the rate equation assuming single site adsorption or competitive adsorption of oleic acid with dissociative adsorption of molecular hydrogen. As presented in **Table S2**, the other rate equations were easily discriminated and disregarded due to negative kinetic constant values and apparent lack of fit with poor linear R^2 regression values < 0.95.

From the comparison between the experimentally obtained data and the predicted results obtained via the rate equations, derived from the L–H surface reaction model including the single site adsorption of tetralin and oleic acid with the dissociative adsorption of molecular H_2 depicted in **Figure 5(a)** and **Figure 5(b)**, an error deviation of less than 20% between the predicted and experimental conversions was obtained. This further signified an excellent correspondence of the fit between the model predictions and experimentally obtained data. Such differences in the error deviation confirmed the kinetic model for both
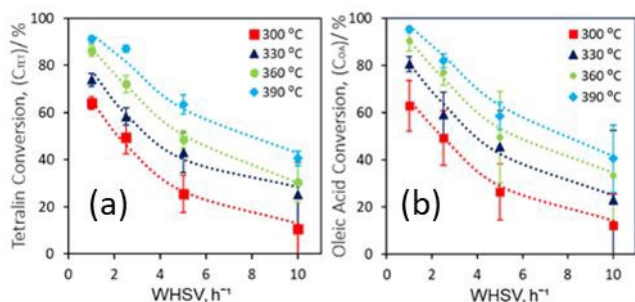
Figure 5: (a) A comparison between experimental data (dots) and predicted (dashed lines) conversion of tetralin obtained from L-H model at reaction temperatures of 300 – 390 °C. (b) A comparison between experimental data (dots) and predicted (dashed lines) conversion of oleic acid obtained from L-H model (Single site, dissociative hydrogen adsorption) at reaction temperatures of 300 – 390 °C.

reactions were able to describe the surface reaction mechanism occurring on the PdCu catalyst very well. In a comparable deoxygenation study, Tian et al. investigated the effect of water and dodecane as hydrogen donor solvents in the catalytic conversion of oleic acid over Pt/C catalysts at 350 °C.[23] It was also reported that both H donor solvent molecules were likely to compete for active sites with oleic acid and effect the rate of reaction adversely.[23]

This corresponds well with our kinetic findings of competitive adsorption of oleic acid, where the unsaturated fatty acid substrate is competing for the same active site with the aromatic ring and H atoms. The dissociative adsorption of H_2 over PdCu catalysts also confirmed and corroborated with many previous kinetic findings reported in the literature.[24-27] Molecular hydrogen was reported extensively in the literature to adsorb onto platinum Group Metal (PGM) based catalysts, especially Pd and Pt with dissociation.[12]

Figure 6 illustrates the reaction scheme for dehydrogenation of tetralin (**Reaction 1**) and deoxygenation of oleic acid (**Reaction 2**). The mechanistic steps for both **Reaction 1** and **2** are listed as follows:

Reaction 1 – Catalytic dehydrogenation of tetralin
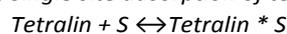
(a) Single site adsorption of tetralin:
    *Tetralin + S ↔Tetralin * S*
(b) Surface reaction – Dehydrogenation of tetralin:
    *Tetralin * S ↔ Naphthalene * S + 4H * S*
(c) Desorption of naphthalene from active site:
    *Naphthalene * S ↔ Naphthalene + S*
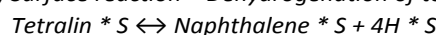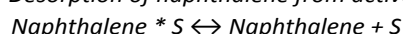
Reaction 2 – Catalytic deoxygenation of oleic acid

(a) Single site adsorption of oleic acid (OA) on active site:
    *OA + S ↔ OA * S*
(b) Surface reaction – Hydrogenation of oleic acid to stearic acid (SA) with dissociative hydrogen atoms liberated from tetralin:
    *OA * S + 2H * S ↔SA * S + 2S*
(c) Surface reaction – Decarboxylation of stearic acid to heptadecane:
    *SA * S ↔ C17 * S + CO2*
(d) Desorption of heptadecane from active site:
    *C17 * S ↔ C17 + S*
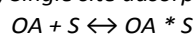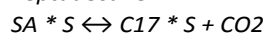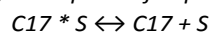
Where S is denoted as an active site on the $Pd_{60}Cu_{40}$ catalyst.

With regard to the role of Pd and Cu active sites in the dehydrogenation and deoxygenation reactions, it can be proposed that both Pd and Cu have an analogous role in catalysing **Reactions 1** and **2**. Such justifications are supported by our previous batch reactions,[4] where both Pd and Cu materials were found to be active for dehydrogenation of tetralin (Pd being the most active). Similarly, both metals are also active in the deoxygenation of
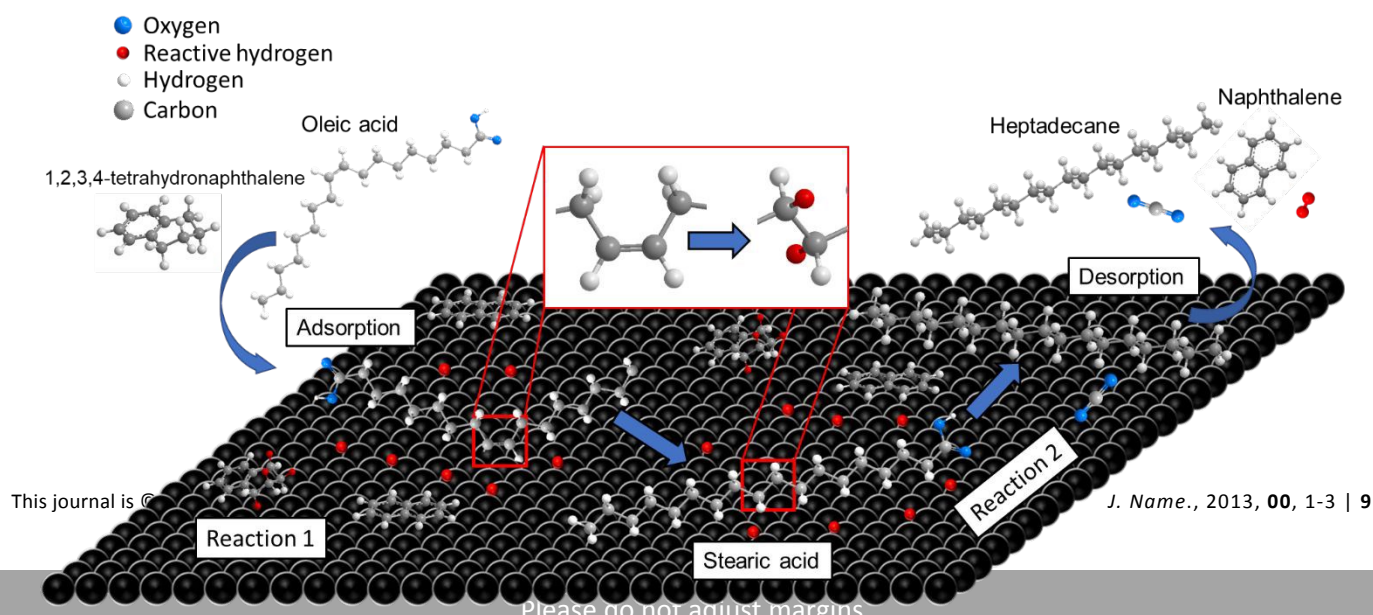
Figure 6: General mechanistic scheme for dehydrogenation of tetralin and deoxygenation of oleic acid. Black balls signify the $Pd_{60}Cu_{40}$ alloyed surface for single site adsorption.

oleic acid, although exhibiting different selectivities. These observations show that both **Reaction 1** and **2** can be catalysed by Pd and Cu, suggesting that the same active sites are responsible for both reactions. This is in good agreement with the previous studies reported by Shafaghat, et al, where both the reactions of hydrogen liberation from a H donor molecule and hydrogen consumption by the acceptor molecule should occur on the same active site.[28]

Determination of activation energies and rate controlling step

Figure 7(a) and **Figure 7(b)** illustrate the Arrhenius plots of the catalytic dehydrogenation of tetralin (**Reaction 1**) and catalytic deoxygenation of oleic acid (**Reaction 2**), respectively. To determine the activation energy and pre-exponential factor, Arrhenius plots of ln(k) against 1/T were plotted using the predicted rate constants at reaction temperatures between 300–390 ^{o}C, as shown in **Figures 7(a)** and **7(b)**. The activation energy and pre-exponential factor of both reactions was then obtained from the slope and intercept of the Arrhenius plots.

From **Figures 7(a)** and **7(b)**, one can observe that the rate constants of both **Reaction 1** and **2** are in accord to the Arrhenius temperature-dependence relationship, evidenced
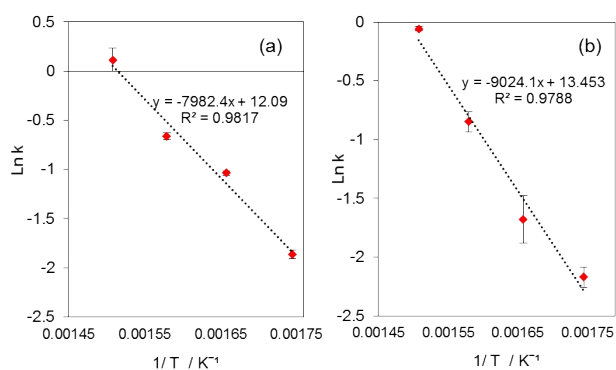
Figure 7: (a) Arrhenius plot for the rate constants of the catalytic dehydrogenation of tetralin over the PdCu catalyst (**Reaction 1**), (b) Arrhenius plot for the rate constants of catalytic deoxygenation of oleic acid over the PdCu catalyst (**Reaction 2**).

from the R^2 values close to unity. The activation energies of **Reaction 1** and **2** were found to be 66.4 $\pm$ 2.7 kJ mol^{-1} and 75.0 $\pm$ 5.1 kJ mol^{-1}, respectively. With the activation energy of **Reaction 2** being evidently higher than that of **Reaction 1**. It can be concluded the single site adsorption or competitive adsorption of oleic acid with dissociative adsorption of molecular H_2 is the rate controlling step, compared to the

dehydrogenation of tetralin. It is noticeable that the rate constant of **Reaction 2** was noticeably larger than the rate constant of **Reaction 1** across all reaction temperatures investigated. This highlighted that the dehydrogenation of tetralin is comparably favourable and faster than the hydrogenation of oleic acid to stearic acid. With that, it further strengthened and reinforced our current kinetic findings that the hydrogenation of oleic acid to stearic acid (**Reaction 2**) is the rate-limiting step.

Table 3 compares the values of activation energy of oleic acid deoxygenation reported previously in the literature. Popov and Kumar developed an empirical kinetic model for the HDO of oleic acid over activated carbon,[29] the activation energy was estimated to be 120 kJ mol^{-1} in a continuous flow process. Hossain, et al. studied the decarboxylation of oleic acid in a batch hydrothermal reactor over activated carbon and reported the activation energy to be 90.6 kJ mol^{-1}.[30] Both of the activation energies reported in Popov and Kumar and Hossain, et al.[29, 30] are higher than the activation energy obtained in this study. This is expected since the Pd$_{60}$Cu$_{40}$/C catalyst is more active than the bare carbon support alone. Our previous batch experiments also confirmed that the bare support material did not catalyse **Reaction 1** or **2** considerably.[4] Ayodele, et.al conducted another kinetic study on the HDO of oleic acid using an in-house synthesized fluro-molybdenum-oxalate zeolite supported catalyst and the activated energy was reported to be 98.7 kJ mol^{-1}.[11] In another deoxygenation study by Raut and co-workers, the activation energies of Pd/SBA-12 and Pd/SBA-16 catalysts were reported to be 130.1 kJ mol^{-1} and 127.1 kJ mol^{-1}, respectively.[31] Compared to the activation energies reported in Ayodele and Raut, the activation energy required for performing the catalytic deoxygenation of oleic acid over bimetallic Pd$_{60}$Cu$_{40}$/C is considerably lower.[11, 31] This can be explained by the lower sensitivity of the present process to reaction temperature and improved activity performance of bimetallic PdCu based catalysts via the synergetic effect between Pd and Cu active sites. Furthermore, introduction of tetralin as an alternative H_2 source offers a better solubility of H_2 within the reaction mixture, which successively enhanced the diffusional mass transfer of hydrogen in the deoxygenation reaction.

Table 3: Comparison of activation energy of oleic acid deoxygenation reported in the literature.

Reactant	Catalyst	Reaction conditions	Activation energy (kJ mol^{-1})	Reference
Oleic acid	Activated carbon	350–380 ^{o}C / 24.1 MPa	120.0	[29]
Oleic acid	Activated carbon	350-400 ^{o}C / 15.1 MPa	90.6	[30]

Oleic acid	FMoOx/Zeolite	320-360 ^{o}C / 2 MPa	98.7	11
Oleic acid	Pd/SBA-12	300-325 ^{o}C / 1 MPa	130.1	31
	Pd/SBA-16		127.1	
Oleic acid	Pd60Cu40/C	300-390 ^{o}C / 1 MPa	75.0 ± 5.1	This work

Conclusions

The hydrodeoxygenation of oleic acid, a model compound for fatty acid wastes, using tetralin as a hydrogen-donor solvent in the presence of a bimetallic PdCu/C catalyst under continuous flow was investigated. Under optimum conditions (360 °C and a WHSV of 1 h^{-1}) C$_{17-18}$ selectivity of 81% was achieved. In order to gain an in-depth mechanistic insight of the tandem hydrogen transfer and deoxygenation reactions, a comprehensive kinetic modelling study was performed considering different reaction temperatures (300–390 ^{o}C) and WHSVs (1–10 h^{-1}). Kinetic studies showed that data obtained from the dehydrogenation of tetralin, **Reaction 1**, was well fitted by the rate equation derived from the L–H model, assuming the surface reaction as rate controlling step. Furthermore, the experimental data obtained from the deoxygenation of oleic acid, **Reaction 2**, was best fitted by the rate equation derived from the L–H model assuming single site adsorption of oleic acid with the dissociative adsorption of molecular H$_2$. Based on the Arrhenius plots, the activation energy of **Reactions 1** and **2** were found to be 66.4 $\pm$ 2.7 kJ mol^{-1} and 75.0 $\pm$ 5.1 kJ mol^{-1}, respectively. Based on the activation energies of **Reaction 1** and **2**, it is concluded that the single site adsorption or competitive adsorption of oleic acid with dissociative adsorption of H$_2$ is the rate controlling step, this is apparent from the higher activation energy required for **Reaction 2**. In terms of the individual role of active sites (Pd & Cu) in the catalytic deoxygenation reaction, both Pd and Cu have an analogous role in **Reactions 1** and **2**. In summary, the kinetic models presented in this work can be used for preliminary reactors design and sizing as well as techno-economic analysis of synthetic diesel fuel production from fatty acid model compounds.

Conflicts of interest

There are no conflicts to declare

Acknowledgements

References

1. R. Elkacmi, N. Kamil, M. Bennajah and S. Kitane, *Biomed Res Int*, 2016, **2016**, 1397852.
2. C. D. Amorim, A. G. Camilo, C. de Oliveira, M. E. Petenucci and G. G. Fonseca, *Sustainable Materials and Technologies*, 2015, **6**, 1-5.
3. L. Boda, G. Onyestyák, H. Solt, F. Lónyi, J. Valyon and A. Thernesz, *Applied Catalysis A: General*, 2010, **374**, 158-169.
4. K. W. Cheah, M. J. Taylor, A. Osatiashtiani, S. K. Beaumont, D. J. Nowakowski, S. Yusup, A. V. Bridgwater and G. Kyriakou, *Catalysis Today*, 2019, DOI: 10.1016/j.cattod.2019.03.017.
5. M. Snåre, I. Kubičková, P. Mäki-Arvela, D. Chichova, K. Eränen and D. Y. Murzin, *Fuel*, 2008, **87**, 933-945.
6. J. G. Immer and H. H. Lamb, *Energy & Fuels*, 2010, **24**, 5291-5299.
7. M. Arend, T. Nonnen, W. F. Hoelderich, J. Fischer and J. Groos, *Applied Catalysis A: General*, 2011, **399**, 198-204.
8. S. A. Hollak, M. A. Ariens, K. P. de Jong and D. S. van Es, *ChemSusChem*, 2014, **7**, 1057-1062.
9. C. Wang, Q. Liu, J. Song, W. Li, P. Li, R. Xu, H. Ma and Z. Tian, *Catalysis Today*, 2014, **234**, 153-160.
10. P. Kumar, S. R. Yenumala, S. K. Maity and D. Shee, *Applied Catalysis A: General*, 2014, **471**, 28-38.
11. O. B. Ayodele, H. U. Farouk, J. Mohammed, Y. Uemura and W. M. A. W. Daud, *Journal of the Taiwan Institute of Chemical Engineers*, 2015, **50**, 142-152.
12. L. Zhou and A. Lawal, *Applied Catalysis A: General*, 2017, **532**, 40-49.
13. K. W. Cheah, S. Yusup, G. Kyriakou, M. Ameen, M. J. Taylor, D. J. Nowakowski, A. V. Bridgwater and Y. Uemura, *International Journal of Hydrogen Energy*, 2019, **44**, 20678-20689.
14. Z. Niu and Y. Li, *Chemistry of Materials*, 2013, **26**, 72-83.
15. A. D. Jewell, E. C. Sykes and G. Kyriakou, *ACS Nano*, 2012, **6**, 3545-3552.
16. A. S. Abbas, T. M. Albayati, Z. T. Alismaeel and A. M. Doyle, *Iraqi Journal of Chemical and Petroleum Engineering*, 2016, **17**, 47-60.
17. L. N. Silva, I. C. P. Fortes, F. P. de Sousa and V. M. D. Pasa, *Fuel*, 2016, **164**, 329-338.
18. N. Joshi and A. Lawal, *Industrial & Engineering Chemistry Research*, 2013, **52**, 4049-4058.
19. O. B. Ayodele, O. S. Togunwa, H. F. Abbas and W. M. A.

W. Daud, *Energy Conversion and Management*, 2014, **88**, 1104-1110.

20. S. Gong, A. Shinozaki and E. W. Qian, *Industrial & Engineering Chemistry Research*, 2012, **51**, 13953-13960.

21. Ł. Jęczmionek and K. Porzycka-Semczuk, *Fuel*, 2014, **131**, 1-5.

22. A. Srifa, K. Faungnawakij, V. Itthibenchapong, N. Viriya-Empikul, T. Charinpanitkul and S. Assabumrungrat, *Bioresour Technol*, 2014, **158**, 81-90.

23. Q. R. Tian, Z. H. Zhang, F. Zhou, K. Q. Chen, J. Fu, X. Y. Lu and P. K. Ouyang, *Energy & Fuels*, 2017, **31**, 6163-6172.

24. J. R. Boes, G. Gumuslu, J. B. Miller, A. J. Gellman and J. R. Kitchin, *ACS Catalysis*, 2015, **5**, 1020-1026.

25. M. Hronec, K. Fulajtárová, I. Vávra, T. Soták, E. Dobročka and M. Mičušík, *Applied Catalysis B: Environmental*, 2016, **181**, 210-219.

26. C. M. Kruppe, J. D. Krooswyk and M. Trenary, *The Journal of Physical Chemistry C*, 2017, **121**, 9361-9369.

27. M. J. Taylor, L. J. Durndell, M. A. Isaacs, C. M. A. Parlett, K. Wilson, A. F. Lee and G. Kyriakou, *Applied Catalysis B: Environmental*, 2016, **180**, 580-585.

28. H. Shafaghat, P. S. Rezaei and W. M. A. W. Daud, *Journal of the Taiwan Institute of Chemical Engineers*, 2016, **65**, 91-100.

29. S. Popov and S. Kumar, *Energy & Fuels*, 2015, **29**, 3377-3384.

30. M. Z. Hossain, A. K. Jhawar, M. B. I. Chowdhury, W. Z. Xu, W. Wu, D. V. Hiscott and P. A. Charpentier, *Energy & Fuels*, 2017, **31**, 4013-4023.

31. R. Raut, V. V. Banakar and S. Darbha, *Journal of Molecular Catalysis A: Chemical*, 2016, **417**, 126-134.

Reaction Chemistry & Engineering Accepted Manuscript

ARTICLE